Interdisciplinary Studies on Environmental Chemistry—Marine Environmental Modeling & Analysis, Eds., K. Omori, X. Guo, N. Yoshie, N. Fujii, I. C. Handoh, A. Isobe and S. Tanabe, pp. 239–249.

Formulation of Leeway-Drift Velocities for Sea-Surface Drifting-Objects Based on a Wind-Wave Flume Experiment

Atsuhiko ISOBE[1], Hirofumi HINATA[2], Shin'ichiro KAKO[1] and Shun YOSHIOKA[3]

[1]*Center for Marine Environmental Studies, Ehime University, 2-5 Bunkyo-cho, Matsuyama 790-8577, Japan*
[2]*National Institute for Land and Infrastructure Management, 3-1-1 Nagase, Yokosuka 239-0826, Japan*
[3]*Department of Earth System Science and Technology, Kyushu University, 6-1 Kasuga-Koen, Kasuga 816-8580, Japan*

(Received 30 October 2010; accepted 20 December 2010)

Abstract—A leeway-drift velocity formula is provided for practical use to trace drifting objects on the sea surface, based on a laboratory experiment using a wind-wave flume. In general, the difficulty arises mainly from the square root of drag coefficients between the air and seawater (R_C). In the laboratory experiment, drift velocities of spheres and circular cylinders were measured in wind-wave flume under various wind speeds to determine the R_C value reasonably. As a result, the R_C value is able to be approximated to 1.1×10^{-5} R_{ea}, where R_{ea} denotes the Reynolds number on the air side of drifting objects.

Keywords: leeway drift, drifting object, wind-wave flume experiment

INTRODUCTION

Wind-induced drag force exerted on objects floating on the sea surface causes motion relative to ocean currents (i.e., leeway drift; Fig. 1). An equilibrium state is accomplished on a relatively short timescale between the wind-induced drag force ($\rho_a Cd_a W|W|$) and current-induced one ($\rho_s Cd_s U|U|$) on the floating objects (Anderson *et al.*, 1998), so a straightforward equation available for computing leeway-drift velocities (U) is as follows:

$$U = \sqrt{\frac{\rho_a}{\rho_s}} \sqrt{\frac{A_a}{A_s}} \sqrt{\frac{Cd_a}{Cd_s}} W = R_\rho R_A R_C W, \tag{1}$$

where ρ, A, Cd, and W denote the fluid density, projected area of the objects, drag coefficient, and wind speed, respectively, and subscripts a and s denote the parameters in the air and seawater. The former two R coefficients in (1) can be determined *a priori* because spatiotemporal variations of both air and seawater densities play a minor role to determine the leeway drift, and because projected

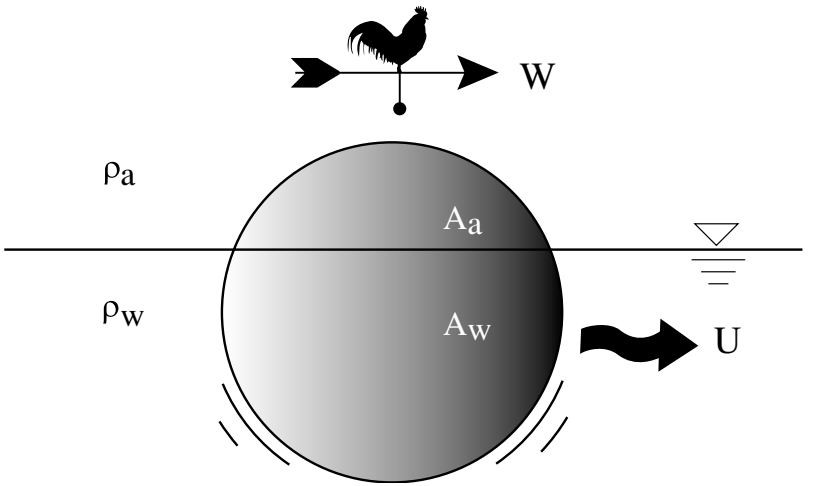

Fig. 1. Drifting object on the sea surface and parameters used in (1).

areas are able to be roughly estimated using the specific gravity of drifting objects.

The difficulty arises mainly from the third R, that is, the square root of the drag-coefficient ratio between the air and seawater. It is well known that drag coefficients suddenly decrease when Reynolds numbers around flow-past objects exceed their critical values (e.g., 3.38×10^5 for rigid spheres; see Fig. 2 in the present paper, and table 5.2 in Clift *et al.*, 1978). Nevertheless, in general, the ratio is set to be unity (e.g., Richardson, 1997; Anderson *et al.*, 1998) because Reynolds numbers above the sea surface are assumed to be close to those in seawater. Besides, the ratio is set to be an adjustable constant in considering motion of drifters composed of a single buoy and drogue for the scientific use (Geyer, 1989; Edwards *et al.*, 2006). We next estimate a typical value for drifting objects using the 10 m/s wind speed (W), 1-m diameter (D) sphere, and 0.1-m/s leeway-drift velocity (U). Using kinetic viscosities of the air ($\nu_a = 1.8 \times 10^{-5}$ m^2/s) and water ($\nu_s = 10^{-6}$ m^2/s), one can find that the Reynolds number exceeds the critical value only on the air side, and that R_C takes a value less than unity. When Reynolds numbers in the air are larger than those in seawater in the actual ocean, as the situation mentioned above, leeway-drift velocities must be lower than we have evaluated using (1) with R_C of unity. The present study provides a leeway-drift velocity formula with an appropriate R_C value for practical use, based on a laboratory experiment using a wind-wave flume.

EXPERIMENTAL PROCEDURE

The laboratory experiment to measure leeway-drift velocities of various samples was carried out under various wind-speed conditions in a wind-wave

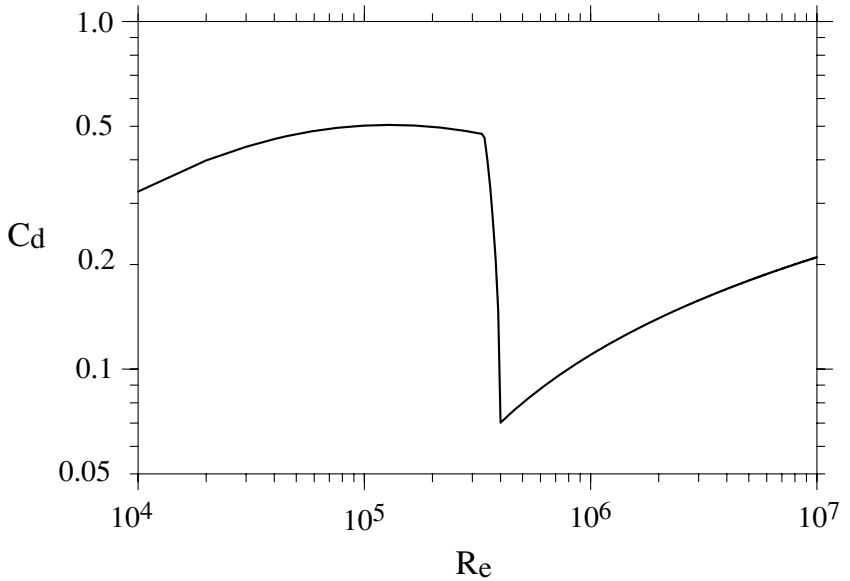

Fig. 2. Relationship between Reynolds number (Re) and drag coefficient (Cd) around flow-past spheres. The formulae in table 5.2 of Clift *et al*. (1978) are used to depict this curve.

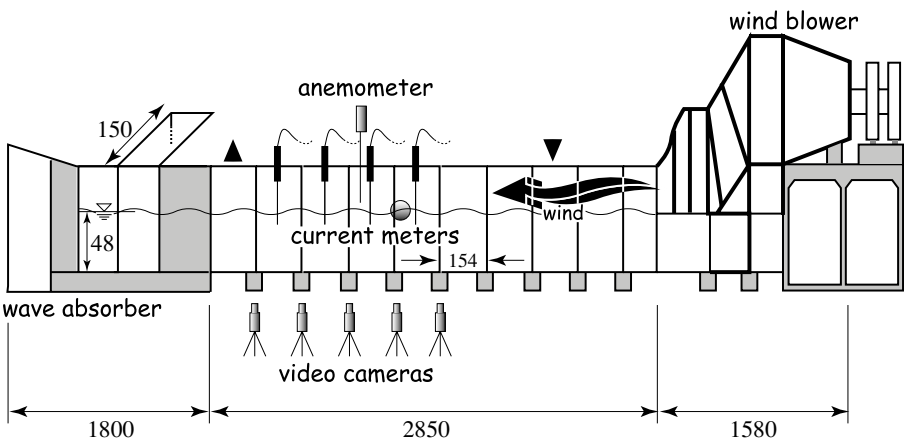

Fig. 3. Wind-wave flume used in the present study. The unit of digits is in centimeters.

flume (Fig. 3). The samples a–g (Fig. 4 and Table 1) released at the flume upstream (the reversed triangle in Fig. 3) were carried leftward in the figure by both ambient wind-driven currents and leeway drift forced directly by the winds generated at the wind blower. The symmetrically shaped samples were chosen so

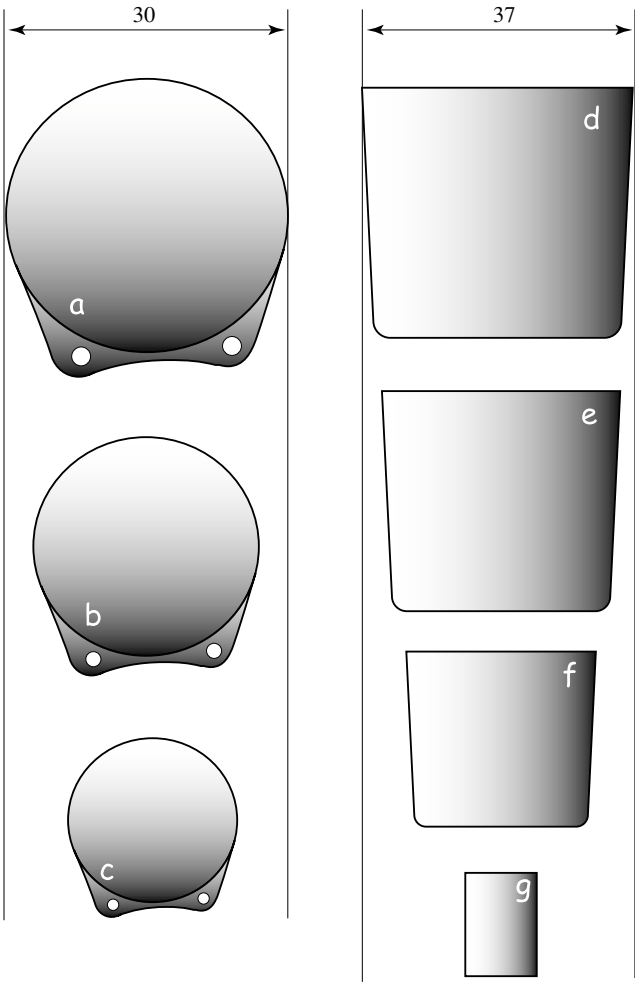

Fig. 4. Size (cm) and shape of the samples (spheres a–c and circular cylinders d–g; see Table 1).

that the cross-wind (lift) component of motion becomes negligible in the course of the experiments. The samples were released after the sufficient time for winds and ambient currents to reach a quasi-steady state. The samples were thereafter picked up at the flume end (triangle in Fig. 3). The top of the wind-wave flume was covered with wood boards in the course of the experiment.

The computation procedure of leeway-drift velocities is as follows. Drift velocities are defined as the sample speed averaged in a "segment" between neighboring flume frames with a 154-cm interval, and were first computed using elapsed times taken for the samples to pass over each segment. The elapsed times

Table 1. Samples and data amount under four wind-speed conditions.

No. (Fig. 4)	Shape	Diameter	Height	$\sqrt{Aa / As}$	Data amount (wind speed between 0 and 0.1 m; m/s)				
					3.2	6.1	7.6	8.4	total
1 (b)	sphere	240	—	2.00	12	8	9	0	29
2 (b)	sphere	240	—	1.47	12	8	10	0	30
3 (b)	sphere	240	—	1.00	9	8	15	0	32
4 (b)	sphere	240	—	0.64	9	8	11	0	28
5 (a)	sphere	300	—	0.99	10	7	10	9	36
6 (c)	sphere	180	—	1.00	11	7	10	0	28
7 (d)	cylinder	369/337	345	1.11	0	14	11	0	25
8 (e)	cylinder	321/296	305	0.95	0	10	12	0	22
9 (f)	cylinder	258/235	240	0.85	0	11	11	0	22
10 (g)	cylinder	100	140	0.77	12	13	17	0	42
				total	75	94	116	9	294

were measured using five digital video cameras (CANON, DC40) in front of each flume frame; the cameras recorded the time at which the samples pass at each frame position with a resolution of 1/100 s. Simultaneously, ambient-current velocities were measured with the interval of 0.1–0.2 s using four current meters (JFE-ALEC, ACM3RS) at the midpoint between the flume frames, at the center of the flume width, and at the 0.1-m depth below the surface of water under the calm condition. The ambient current velocities (typically 0–0.1 m/s) must be removed from the sample drift velocities (typically 0.1–1 m/s) to convert them into velocities due to the leeway drift defined as motion relative to the ambient currents. The measured ambient-current velocities were averaged over the course of the time taken for the samples to pass over each segment. In total, four leeway-drift velocities were obtained for a sample passing over four segments in a single experiment run. However, when the samples collided with the sidewalls and/or current meters in a segment, the drift velocity measured in the segment is not used for subsequent analyses.

Sample sizes, the data amount obtained successfully in the experiments without the collision, and R_A (i.e., the squared projected-area ratio between the air and water) in (1) for all samples are listed in Table 1. The R_A values for the samples except for the spheres 1, 2, and 4 were adjusted to be close to unity by injecting water to the sample interior. The above three spheres were used for investigating the leeway-drift dependence on R_A. Wind speeds at various heights were measured using an anemometer (KANOMAX, model 6531) before experiments were carried out under different wind speed conditions (Fig. 5). The digits in Table 1 denote the wind speed averaged vertically below the 0.1-m height; the averaged speeds are computed using logarithmic curves fitted by a least square method, and the 0.1-m height is chosen for the typical height of the sample surface exposed in the air.

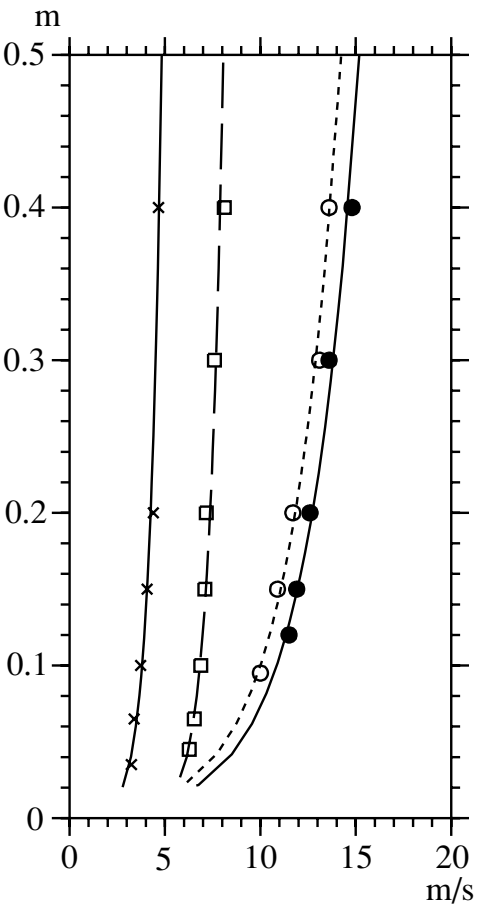

Fig. 5. Vertical wind profiles in the experiment. The crosses, squares, open and solid circles are used for experiment runs with the wind speeds, 3.2, 6.1, 7.6, and 8.4 m/s, respectively, averaged between 0 and 0.1-m height using the logarithmic curves fitted to the marks with a least square method.

RESULTS

First, the dependence of leeway-drift velocities on wind speeds is investigated (Fig. 6). It is reasonable that leeway-drift velocities increase as wind speeds increase, and that samples with the large projected area in the air (i.e., the large R_A in (1)) have large leeway-drift velocities. In fact, the dependence of the leeway-drift velocities on R_A is clearly seen in Fig. 6. For instance, the leeway-drift velocities for the spheres with R_A of 2.0 (open circles) are all larger than those with 0.99–1.47 R_A (small open circles). In addition, the spheres with 0.64 R_A (solid circles) mostly have the leeway-drift velocities smaller than those of the

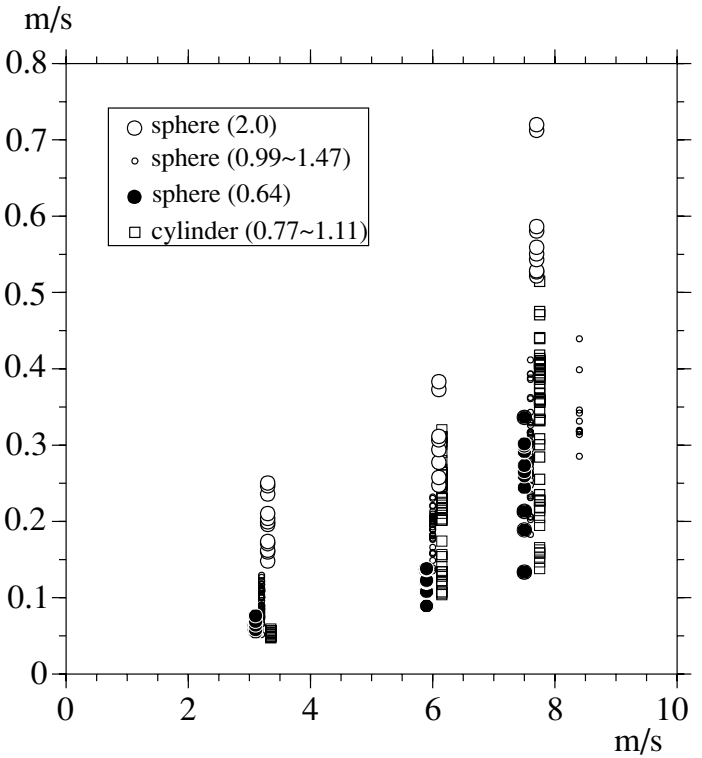

Fig. 6. Scatter plot of drift velocities (ordinate) defined in the text versus wind speeds (abscissa). The velocities for the spheres and cylinders are plotted using the marks shown in the upper-left corner of this figure. The digits in the parentheses denote R_A in (1) and Table 1. The marks with the same wind speeds are slightly shifted laterally for ease of reference in the figure.

spheres with larger R_A values. It is however difficult to distinguish the leeway-drift velocities of spheres from those of cylinders because the velocities of the cylinders increase with the wind speed in the same manner as those of the spheres. It is noted that the leeway-drift velocities for the samples with the same R_A value become widely scattered as the wind speed increases, although (1) states that leeway-drift velocities are merely proportional to the wind speed if three R coefficients take constant values. It is therefore suggested that R_C in (1) disperses widely as the wind speed increases in the experiment.

Drag coefficients (hence, R_C values) depend on Reynolds numbers, not only on the wind speeds, so the leeway-drift velocities are plotted against the Reynolds number in water (Fig. 7; $R_{es} = UD/\nu_s$, where D denotes the sample diameter in Table 1). The velocities are normalized by those computed using (1) with R_C of unity. The Reynolds numbers in the air ($R_{ea} = WD/\nu_a$) are larger than those in water in the present experiment (Fig. 8), and so the Reynolds number in the air

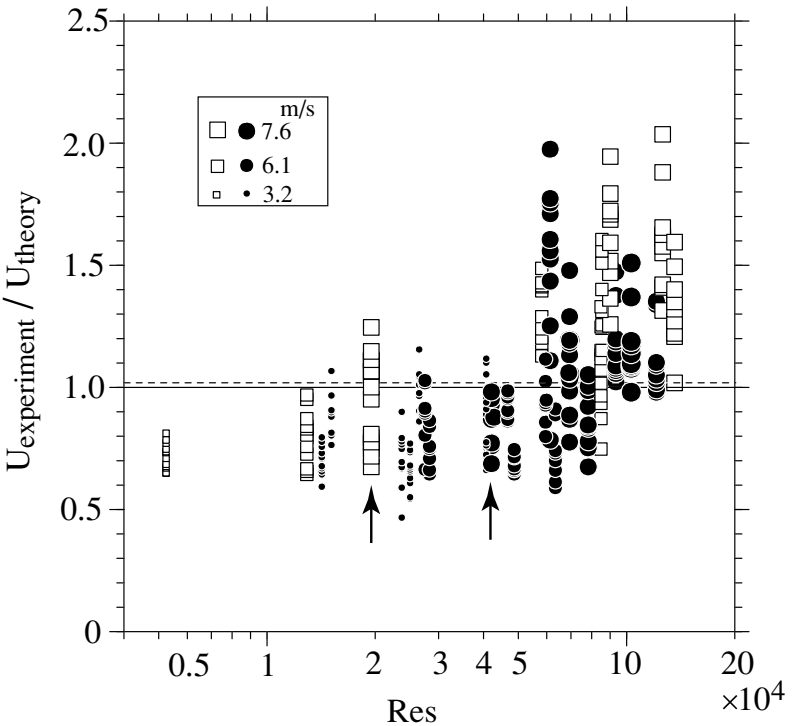

Fig. 7. Scatter plot of leeway-drift velocities (ordinate) versus the Reynolds number in water (R_{es}; abscissa). The leeway-drift velocities are normalized by the theoretical values with R_C of unity in (1). The solid circles and open squares are used for spheres and cylinders, respectively, as shown in the upper left of the figure. The size of the marks denotes the averaged wind speed (Table 1). Two arrows are used in the description in the text. The broken line indicates the average value computed using all plots in the figure.

was likely to exceed the critical value prior to that in water. If this is the case, R_C (hence, the leeway-drift velocity) should decrease suddenly when the Reynolds number in the air exceeds the critical value. However, in fact, the leeway-drift velocities (hence, R_C) rather increase as the Reynolds number increases (Fig. 7); the Reynolds numbers both in the air and water increase in the same manner (Fig. 8), so the increase of the leeway-drift velocities would be seen clearly even if the Reynolds number in the air was used for the abscissa in Fig. 7.

In general, experimental results under the high wind-speed condition are likely to be erroneous because wind waves generated in the flume might disturb sample motion in terms of the wave rectification (Geyer, 1989), the Stokes drift, and so forth; in fact, wind waves were generated over the course of the experiments with the wave height lower than 2.5 cm, wave period shorter than 0.5 s, and wavelength around 50 cm, which were observed in the video-cameras' records. These waves however result in the Stokes drift smaller than 3 cm/s, which is one-

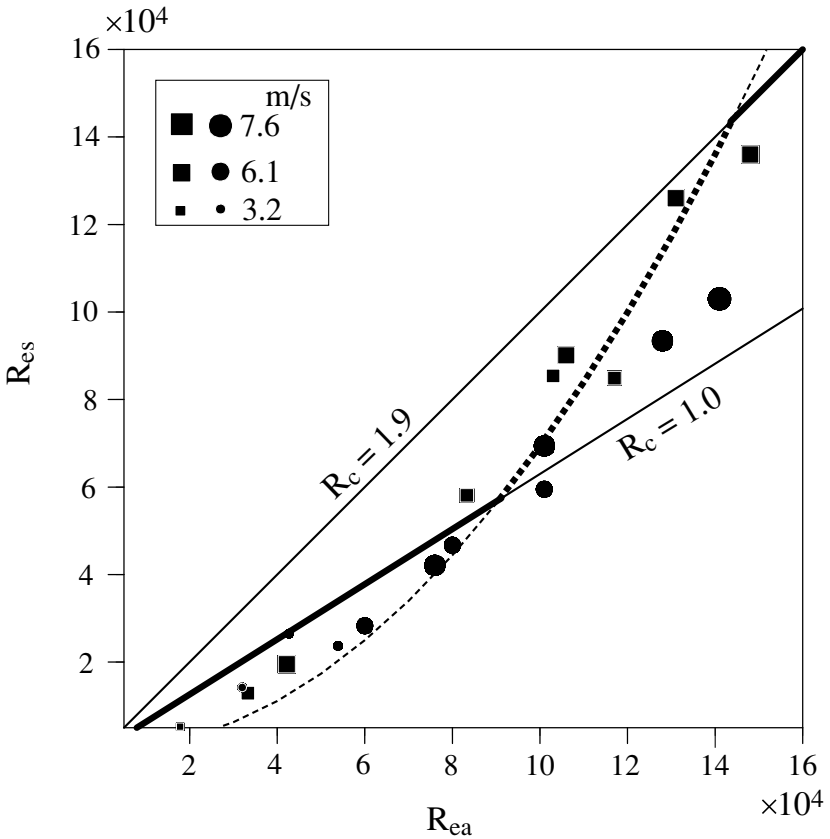

Fig. 8. Scatter plot of Reynolds numbers in the air (abscissa) and water (ordinate). The samples with *Aa/As* of unity are used to depict this figure. Note that the Reynolds numbers averaged using four data in a single experiment run are plotted here. The solid circles and squares are used for spheres and cylinders, respectively, as shown in the upper left of the figure. The size of the marks denotes the averaged wind speed (Table 1). Equation (3) states that the plots should be located close to the lower (upper) line when R_C is equal to unity (1.9). The quadratic equation shown by the broken curve is fitted by a least square method. The approximation along the bold curve is used in the numerical model approach (subsection 4b) in line with (6).

order smaller than drift velocities in Fig. 6. In addition, it is unreasonable to consider that the increase of the leeway-drift velocities at the high Reynolds number results from the contamination due to the wind waves, because the velocities at the low Reynolds number have small values even if the wind speed (hence, wave height) in the flume is highest in the experiments (arrows in Fig. 7). The velocities at the low Reynolds number are smaller than theoretical ones with R_C of unity, presumably due to the fact that the samples did not always move along the flume center where the wind speed was measured, but frequently moved near the sidewalls along which the winds weaken in the boundary layer.

DISCUSSION—FORMULATION OF LEEWAY-DRIFT VELOCITIES—

The objective of the present study is to provide a leeway-drift formula for practical use by finding an appropriate R_C value based on the wind-wave flume experiment. Thus, this paper will not delve into the mechanism why the leeway-drift velocities (hence, R_C) increase with the Reynolds number. Instead, we will refer to Clift *et al.* (1978) and Brucato *et al.* (1998) in which they demonstrate that critical Reynolds numbers and/or drag coefficients, in principal, are either decreased or increased depending on the particular case in turbulent fluid. It is suggested that, in the present experiment, the Reynolds number in water reaches the critical value prior to that in the air because of turbulence induced by wind waves and/or bubbles in water, and so R_C increases as the Reynolds number increases.

Leeway-drift velocities are next formulized using the scatter plot (Fig. 8) between the Reynolds numbers in the air (R_{ea}) and water (R_{es}). Substituting (1) into U for the Reynolds number in water yields

$$R_{es} = \frac{R_\rho R_A R_C W D}{\nu_s}. \tag{2}$$

Using the Reynolds number in the air, (2) can be rewritten as

$$R_{es} = R_\rho R_A R_C \frac{\nu_a}{\nu_s} R_{ea}. \tag{3}$$

The samples with R_A nearly equal to unity (i.e., 3, 5, 6, 7, 8, 9, and 10 in Table 1) are chosen to depict Fig. 8 because we examine how the relationship between R_{es} and R_{ea} depends on R_C. For instance, all plots would be located along the lower line in the figure if R_C were unity. However, in fact, the plots gradually deviate upward from the line as the Reynolds number increases, providing a quadratic equation to approximate the plots as

$$R_{es} = 6.93 \times 10^{-6} R_{ea}^2. \tag{4}$$

Comparing (3) with (4) using the appropriate values for R_ρ (~0.035), R_A (~1.0), ν_a (~1.8×10^{-5} m^2/s) and ν_s (~1.0×10^{-6} m^2/s), we can obtain

$$R_C \approx 1.1 \times 10^{-5} R_{ea}. \tag{5}$$

Substituting the above formulation to R_C in (1) yields the leeway-drift velocity for practical use. In the following application, however, we set the R_C values within the range:

$$1.0 < R_C < R_{C\max}, \tag{6}$$

assuming that the Reynolds number in water always reaches the critical number prior to that in the air (hence, $1.0 < R_C$) because of wind-induced turbulence in water, and that the maximum value ($R_{C\max}$) is determined using the drag-coefficient ratio between the both sides of the critical Reynolds number.

We next examine the object size suitable for adopting (5) in the actual situation. This equation states that the drag-coefficient ratio exceeds unity when objects with the diameter larger than 0.16 m are carried by 10-m/s winds. However, in the 10-m/s wind fields, (5) is unavailable for objects larger than 1 m because the square root of the drag coefficient (R_C) exceeds 6, which is unlikely to stay within the range of (6) for various objects (<1.9 for cylinders, and <~5 for spheres; see Fig. 2). Hence, the leeway-drift velocity proposed in the present study should be adopted for drifting objects with the size ranging roughly from 0.1 meter to one meter, and in the period longer than 5 days in the actual ocean; otherwise R_C of unity is sufficient for computing leeway-drift velocities. Plausible applications of the leeway-drift velocity equation proposed in the present study are for seeking the fate and/or origin of driftwoods, anthropogenic marine litter, and so forth.

Acknowledgments—The National Institute for Land and Infrastructure Management for providing us with the opportunity to conduct the wind-wave flume experiment, JFE-ALEC for providing the current meters (ACM3RS) with an instructor are greatly appreciated. This work was supported by the Global Environment Research Fund (D-071 and B-1007) of the Ministry of the Environment, Japan.

REFERENCES

Anderson, E., A. Odulo and M. Spaulding (1998): Modeling of leeway drift. U.S. Coast Guard Research and Development Center Report, CG-D-06-99.

Brucato, A., F. Grisafi and G. Montante (1998): Particle drag coefficients in turbulent fluids. *Chem. Eng. Sci.*, **53**, 3295–3314.

Clift, R., J. Grace and M. E. Webar (1978): *Bubbles, Drops, and Particles*. Dover Publications, Inc., New York, 381 pp.

Edwards, K. P., F. E. Werner and B. O. Blanton (2006): Comparison of observed and modeled drifter trajectories in coastal regions: an improvement through adjustments for observed drifter slip and errors in wind fields. *J. Atmos. Oceanic Technol.*, **23**, 1614–1620.

Geyer, W. R. (1989): Field calibration of mixed-layer drifters. *J. Atmos. Oceanic Technol.*, **6**, 333–342.

Richardson, P. L. (1997): Drifting in the wind: leeway error in shipdrift data. *Deep-Sea Res.*, **44**, 1877–1903.

A. Isobe (e-mail: aisobe@ehime-u.ac.jp)